Published in final edited form as:
J Nucl Med. 2008 July ; 49(7): 1075–1079. doi:10.2967/jnumed.108.050997.

"MOTION-FROZEN" MYOCARDIAL PERFUSION SPECT IMPROVES DETECTION OF CORONARY ARTERY DISEASE IN OBESE PATIENTS

Yasuyuki Suzuki, MD[1], **Piotr J. Slomka, PhD**[1,2,3], **Arik Wolak, MD**[1], **Muneo Ohba, MD**[1], **Shoji Suzuki, MD**[1], **Ling De Yang, MD**[1], **Guido Germano, PhD**[1,2], and **Daniel S. Berman, MD**[1,2]

[1]Departments of Imaging and Medicine, Cedars-Sinai Medical Center, Los Angeles, CA, USA.

[2]Department of Medicine. David Geffen School of Medicine at UCLA, Los Angeles, CA.

Abstract

We recently reported that motion-frozen (MF) computer technique improved image quality of myocardial perfusion SPECT without sacrificing count density by reconstruction of perfusion images with all counts shifted to end diastolic (ED) frame. In this study, we aimed to compare diagnostic performance of the standard and motion-frozen processing using quantitative analysis in obese patients.

Methods—Patients with known coronary artery disease (CAD) were excluded. We studied 90 consecutive obese patients (Body Mass Index 30.1–46.8, average 34.3±3.6), age 63±12 years, 30% female, who underwent both standard supine rest ^{201}Tl/stress ^{99m}Tc dual isotope gated myocardial perfusion SPECT and cardiac catheterization within 3 months. Motion-frozen images were obtained from non-linear image warping of images from all phases to the ED position. Total perfusion deficit (TPD) was defined as a product of defect extent and severity for standard supine (S-TPD) and motion-frozen (MF-TPD) datasets with the use of gender-specific standard and MF normal limits. We compared the sensitivity, specificity and receiver operator characteristic curves (ROC) obtained from S-TPD and MF-TPD.

Results—The area under the curve for MF-TPD was significantly larger than for S-TPD for the detection of CAD (≥70% stenosis) (0.93±0.25 vs 0.88±0.32, $p<0.05$). In 7/31 patients without CAD, MF analysis corrected false positive non-MF results. While sensitivity was the same [93% vs 95% for S-TPD and MF-TPD respectively (p=NS)], MF-TPD had higher specificity (77% vs. 55%) and accuracy (89% vs. 80%) (both $p<0.05$) than S-TPD.

Conclusion—Motion-frozen processing of myocardial SPECT imaging improves accuracy of CAD detection in obese patients.

Keywords

gated SPECT; myocardial perfusion; image registration; image warping; coronary artery disease; motion correction

INTRODUCTION

We have previously shown that it is feasible to correct gated myocardial perfusion SPECT (MPS) for cardiac motion using motion-frozen (MF) technique (1). This technique tracks the

Corresponding Author/ Reprint Requests: Piotr Slomka; Cedars-Sinai Medical Center. Department of Imaging. #A047 8700 Beverly Blvd, Los Angeles, 90048, CA. USA. Piotr.Slomka@cshs.org Tel:1-310-423-4348 Fax: 310-423-0173.

left ventricle through all cardiac phases and subsequently shifts the counts from most of the cardiac cycle (excluding the systolic phase) to the end diastolic (ED) position by means of non-linear image warping. Such warped images are summed to provide MF MPS images in ED phase. We have shown that with the MF approach we can obtain higher quality images as compared to the standard summation of gated frames (1).

In obese patients, image quality of summed perfusion images is often problematic due to count-poor perfusion images in each phase and blurring caused by cardiac motion associated with potential differences between systolic and diastolic phase photon attenuation. Therefore, we hypothesized that the use of MF technique in the obese population with Body Mass Index (BMI) ≥30 could improve the diagnostic performance of quantitative MPS for detection of coronary artery disease (CAD).

MATERIALS AND METHODS

Patient Population and Acquisition Protocols

Normal Database Population—Normal limits were obtained retrospectively from a group of 80 patients (40 females, 40 males) with very low likelihood of CAD (< 5 %) (Table 1), who had no history of CAD, no diabetes, no symptoms of typical angina or shortness of breath, normal resting ECG and non-ischemic stress ECG response, and normal stress and rest gated MPS images. Stress acquisition was performed with either exercise or adenosine stress. Separate male and female normal limits were created for standard summed perfusion data and motion-frozen MPS data. Gender specific normal limits were created from gated MPS data. All gated studies for MF normal limit were 16-frame gated MPS data. Normal limits were created for the general population and were not BMI-matched; however we have previously shown that normal limits for high and low BMI groups are not significantly different (2).

Test Patient Population—We studied 90 consecutive obese patients (BMI 30.1–46.8, average 34.3±3.6) without known CAD, who underwent both standard supine rest ^{201}Tl/ stress ^{99m}Tc dual isotope gated MPS and cardiac catheterization within 3 months. Clinical characteristics are listed in Table 2. The age of the obese population was 63±12 years, and 30% were female.

Acquisition and Reconstruction Protocols—MPS acquisitions were performed with non-circular orbits, obtaining 64 projections over 180 degrees (45° RAO to 45° LPO) at 25 seconds/projection for ^{99m}Tc sestamibi and 35 seconds/projection for ^{201}Tl images (3). MPS acquisitions were performed by either Philips (Adac Forte or Vertex) or Siemens (e.cam) cameras. All images were subject to standard clinical quality control measures. No attenuation or scatter correction was used. After reconstruction of gated data with filtered back projection (FBP), image reconstruction was performed with Butterworth filter (cut-off 0.83 cycles/cm, order 5) and short-axis slices were automatically generated (4). Iterative backprojection was performed for summed perfusion data. There were 29 patients who had 16-frame gated MPS in the present study group and 61 had 8-frame gated MPS.

Coronary Angiography—Coronary angiography was performed with the standard Judkins approach, and all coronary angiograms were interpreted visually by two experienced physicians who were unaware of MPS results. Coronary angiographic findings are presented in Table 3.

"Motion-Frozen" Technique

This technique has been described previously (1). In "motion-frozen" technique, derived LV contours {Germano, 1995 #1041} {Germano, 1997 #1038; Germano, 1997 #1037; Germano, 1995 #1041} are used in combination with a thin-plate spline image warping. Image data from the 63% of the cardiac cycle are used excluding 3 phases for 8-frame or 6 phases for 16-frame closest to the end-systolic (ES) phase. These parameters were previously established for optimal image quality {Slomka, 2004 #2}. Nonlinear image warping of selected cardiac phases to the spatial position of the ED phase is subsequently performed based on the 3D displacement vectors {Slomka, 2003 #408}.

Automated Perfusion Quantification—Standard and MF stress perfusion studies were separately quantified with fully automated method by the calculation of total perfusion deficit (TPD) as previously described (9). Summed (S-TPD) and motion-frozen TPD (MF-TPD) were calculated based on gender-specific MF normal limits derived from the same normal population using the current Cedars-Sinai software (10). Normal limits from the low-likelihood patient data and the criteria for abnormality were the same as described previously (11). The same average deviation threshold (3.0) was used for summed and MF images. The MF-TPD parameter was expressed in the same units (percentage of myocardium) as S-TPD.

The 17-segment AHA model (12) was used to display the quantitative distribution of both summed and MF perfusion studies.

Statistical Analysis

All continuous variables are expressed as a mean ± one standard deviation. Paired *t* tests were used to compare the differences in the paired continuous paired variables. A p-value less than 0.05 was considered significant. For all statistical analysis tasks, we used the Analyze-It software Version 1.71 (Analyze-It Software, Ltd., Leeds, UK). The receiver-operating-characteristic (ROC) curve was created to analyze the diagnostic performance of standard and MF TPD for detection of ≥70% or ≥50% stenosis. Hanley and McNeil method (13) was used for comparing curves, since all the tests are performed on the same subjects. The Analyze-it software generated the ROC curves with 40–50 threshold points depending on the data.

RESULTS

Average computing time for MF image creation was 5.1±2.2 seconds for the 16-frame study with the software implemented in C++ language on Microsoft Windows platform (System: Microsoft Windows XP Professional®, Computer: Intel® Pentium® 4 CPU 2.80GHz, 2 GB of RAM).

In seven out of the 90 patients, which included four 8-frame gated MPS and three 16-frame gated MPS, manual adjustment of the LV contours derived from gated MPS data was required for MF analysis, while 12 ungated LV contours, which included eight 8-frame gated MPS, needed manual contour correction for standard summed perfusion analysis. None of the patients in normal database population required any manual adjustment.

Average segmental count distributions derived from gender-specific normal databases are presented in Figure 1. The average count distributions are significantly different between MF and standard summed analysis in 6 of 17 segments in males and 7 of 17 segments in females. MF normal perfusion distribution in the apex shows decrease in both genders,

while basal anterior, lateral and inferior wall of MF analysis show significant relative count increase in both genders.

The average S- and MF-TPD values in normal and abnormal patients as defined by coronary angiography are shown in Table 4. The TPD values were significantly smaller for MF-TPD as compared to S-TPD in both normal patients and patients with CAD. The ROC curves for detection of CAD by MF-TPD and S-TPD are shown in Figure 2. The respective areas under the ROC curves for S- and MF-TPD for detection of ≥70% stenosis and ≥50% stenosis are presented in Table 5. The areas under the ROC curves for detection of ≥70% stenosis are 0.93±0.025 vs 0.89±0.032 for MF-TPD and S-TPD respectively (p=0.014), implying improved diagnostic accuracy of motion-frozen method. The area under the ROC curve for detection of ≥50% stenosis by MF-TPD was also significantly greater than that of S-TPD (0.94±0.024 vs 0.88±0.033, p=0.006). The diagnostic performance of S-TPD and MF-TPD for detection of ≥50% and ≥70% stenosis is presented in Table 6 and 7.

The previously established threshold of 5% for the TPD (9) was applied as the criteria for abnormality. Diagnostic performance using this cutoff value for detection of CAD with ≥50% (A) and ≥70% (B) stenosis criterion is shown in Figure 3. While sensitivity was the same, MF-TPD showed significantly higher specificity ($p<0.05$) resulting in a significant increase in overall accuracy ($p<0.05$). In 6/31 patients without CAD of ≥50% stenosis, MF analysis corrected false positive non-MF results. In 7/31 patients without CAD of ≥70% stenosis, MF analysis corrected false positive non-MF results. Patient characteristics of the cases where false positive S-TPD was corrected by MF-TPD are presented in Table 8. An example of a study in which MF perfusion images correct a false positive finding is shown in Figure 4. These images are from a patient with normal coronary angiography who had an apical defect considered abnormal by S-TPD and normal by MF-TPD.

DISCUSSION

Blurring of summed gated images in the process of forming an “ungated” perfusion image is a source of reduced image quality in MPS. In order to improve the diagnostic performance of nuclear cardiology studies in obese patients, we have applied previously developed MF image technique which reduces image blur due to cardiac motion (1). We have used previously established (9) methods for creating MF normal limits using data derived from gated scans of patients with low likelihood of CAD. We have compared diagnostic performance of MF-TPD and S-TPD with fully automated procedures and demonstrated a significant improvement of specificity and unchanged sensitivity for the MF technique in detection of CAD.

In the present study, majority (67%) of the MPS data of obese patient group were 8-frame gated MPS. Based on the number of the studies which needed the adjustment of the contours, it does not seem that 8-frame gated MPS affect contour detection however in terms of image quality we recommend 16-frame gated study (1).

Count distribution of myocardial perfusion in the normal database derived with MF processing differed from the summed count distribution in the same patients. Relative counts were significantly higher in both genders in basal anterior, lateral and inferior segments while they were significantly lower in both genders in apical segments as compared to standard limits. This reduction of the counts in the apical region in the MF normal database appears to be consistent with the anatomical apical thinning (14) and partial volume effect in the apical segment. Therefore one potential reason for improvement of accuracy by MF processing is more correct depiction of apical thinning in the MF-processed images. On the other hand the increased relative activity in the basal area may be related to the significant

motion of the valve plane along the long axis of the left ventricle and consequently blurred perfusion, resulting in reduced basal counts when ED and ES frames are summed without MF correction.

In the present study, FBP reconstruction was applied to gated data before MF processing and static summed perfusion data were reconstructed with iterative techniques according to our standard protocols. It was impractical to process all gated data with iterative reconstruction since some of the raw gated data was not available. Although FBP is often used in the clinical setting because computational time is shorter, especially for 16-frame gated studies, iterative reconstruction may further add diagnostic advantage to MF analysis because the process of generating projections can incorporate such variables as attenuation, scatter and depth dependent blur (15), which could be seen more in obese patients. Therefore it is likely that the improvement observed with the MF correction of FBP-reconstructed gated data could be further enhanced with the use of iterative reconstruction.

This study has several limitations. In this study, the majority of the patient data had 8-frame gated study and only 29 patients had 16-frame gated study. Iterative reconstruction was not applied to all summed perfusion data, which may potentially result in lower diagnostic performance. MF technique depends on correct contour definition of LV for a gated study and requires visual quality control. Small heart sizes and partial volume effect may reduce image resolution and may lead to lower diagnostic performance of MF image. A relatively small number of cases were analyzed in this study. Only automatic quantitative analysis was used in this study and subjective visual analysis was not performed, therefore the results may reflect the performance in this particular mode only. However, the results obtained in this way are objective and not influenced by observer experience and variability.

CONCLUSION

Quantitative motion-frozen MPS analysis improves detection of CAD in obese patients, through increased specificity. Normal limits of motion-frozen MPS differ from summed perfusion normal limits; therefore, motion-frozen normal limits should be used if quantitation with this motion-frozen approach is employed.

Acknowledgments

This research was supported in part by grants R01HL089765 from the National Heart, Lung, and Blood Institute/ National Institutes of Health (NHLBI/NIH). Its contents are solely the responsibility of the authors and do not necessarily represent the official views of the NHLBI.

REFERENCES

1. Slomka PJ, Nishina H, Berman DS, et al. "Motion-frozen" display and quantification of myocardial perfusion. J Nucl Med. 2004 Jul; 45(7):1128–1134. [PubMed: 15235058]
2. Slomka PJ, Fish MB, Lorenzo S, et al. Simplified normal limits and automated quantitative assessment for attenuation-corrected myocardial perfusion SPECT. J Nucl Cardiol. 2006 Sep; 13(5): 642–651. [PubMed: 16945744]
3. Berman DS, Kiat H, Friedman JD, et al. Separate acquisition rest thallium-201/stress technetium-99m sestamibi dual-isotope myocardial perfusion single-photon emission computed tomography: a clinical validation study. J Am Coll Cardiol. 1993; 22(5):1455–1464. [PubMed: 8227805]
4. Germano G, Kavanagh PB, Chen J, et al. Operator-less processing of myocardial perfusion SPECT studies. J Nucl Med. 1995; 36(11):2127–2132. [PubMed: 7472609]
5. Germano G, Kiat H, Kavanagh PB, et al. Automatic quantification of ejection fraction from gated myocardial perfusion SPECT. J Nucl Med. 1995; 36(11):2138–2147. [PubMed: 7472611]

6. Germano G, Kavanagh PB, Berman DS. An automatic approach to the analysis, quantitation and review of perfusion and function from myocardial perfusion SPECT images. Int J Card Imaging. 1997; 13(4):337–346. [PubMed: 9306148]
7. Germano G, Erel J, Lewin H, Kavanagh PB, Berman DS. Automatic quantitation of regional myocardial wall motion and thickening from gated technetium-99m sestamibi myocardial perfusion single-photon emission computed tomography. J Am Coll Cardiol. 1997; 30(5):1360–1367. [PubMed: 9350940]
8. Slomka PJ, Dey D, Przetak C, Aladl UE, Baum RP. Automated 3-dimensional registration of stand-alone (18)F-FDG whole-body PET with CT. J Nucl Med. 2003; 44(7):1156–1167. [PubMed: 12843232]
9. Slomka PJ, Nishina H, Berman DS, et al. Automated quantification of myocardial perfusion SPECT using simplified normal limits. J Nucl Cardiol. 2005 Jan-Feb;12(1):66–77. [PubMed: 15682367]
10. Germano G, Kavanagh PB, Waechter P, et al. A new algorithm for the quantitation of myocardial perfusion SPECT. I: technical principles and reproducibility. J Nucl Med. 2000 Apr; 41(4):712–719. [PubMed: 10768574]
11. Van Train KF, Areeda J, Garcia EV, et al. Quantitative same-day rest-stress technetium-99m-sestamibi SPECT: definition and validation of stress normal limits and criteria for abnormality. J Nucl Med. 1993; 34(9):1494–1502. [PubMed: 8355069]
12. Cerqueira MD, Weissman NJ, Dilsizian V, et al. Standardized myocardial segmentation and nomenclature for tomographic imaging of the heart: a statement for healthcare professionals from the Cardiac Imaging Committee of the Council on Clinical Cardiology of the American Heart Association. Circulation. 2002 Jan 29; 105(4):539–542. [PubMed: 11815441]
13. Hanley JA, McNeil BJ. A method of comparing the areas under receiver operating characteristic curves derived from the same cases. Radiology. 1983 Sep; 148(3):839–843. [PubMed: 6878708]
14. DePuey EG 3rd. How to detect and avoid myocardial perfusion SPECT artifacts. J Nucl Med. 1994 Apr; 35(4):699–702. [PubMed: 8151397]
15. Hutton BF, Hudson HM, Beekman FJ. A clinical perspective of accelerated statistical reconstruction. Eur J Nucl Med. 1997 Jul; 24(7):797–808. [PubMed: 9211768]

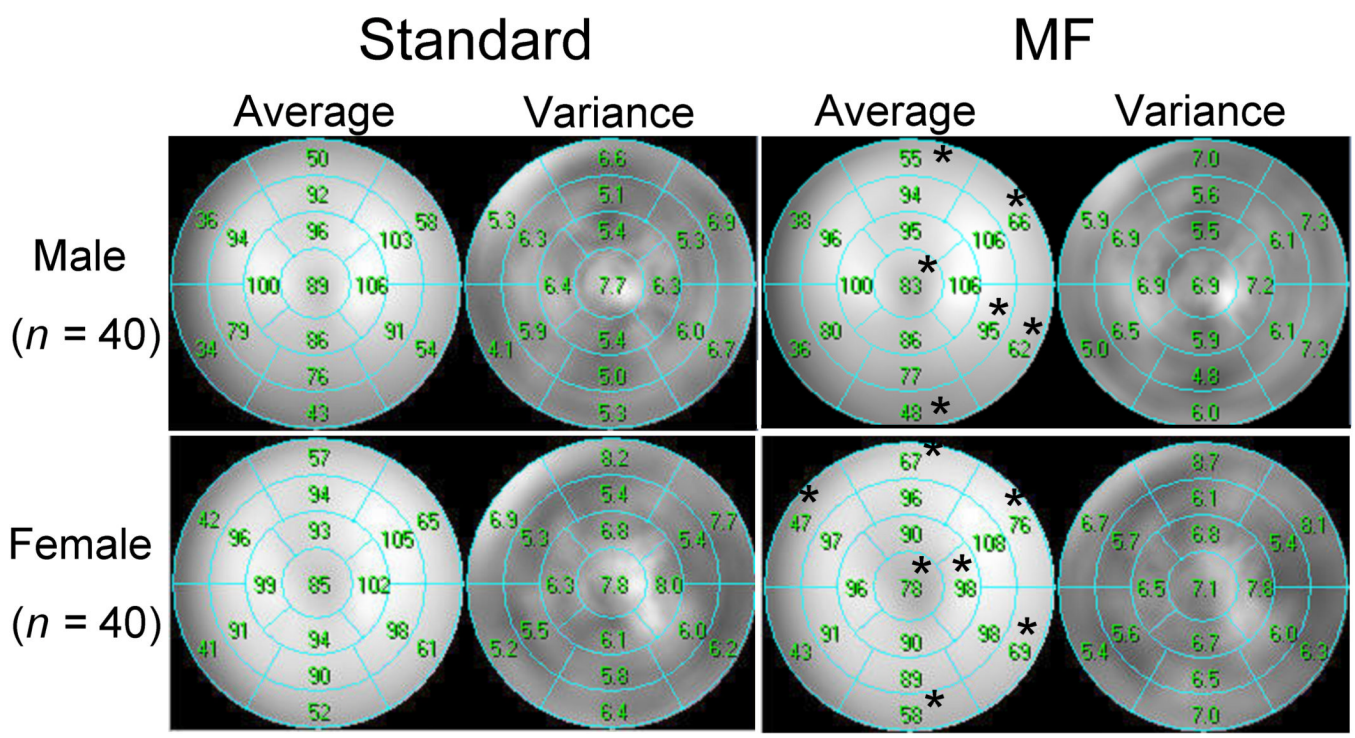

Figure 1.
Segmental comparison of gender-specific standard (left) and motion-frozen (right) mean normal perfusion distribution for males (upper) and females (bottom). Asterisks beside the value of the average % count denote significant differences between standard and motion-frozen analysis ($p<0.05$).

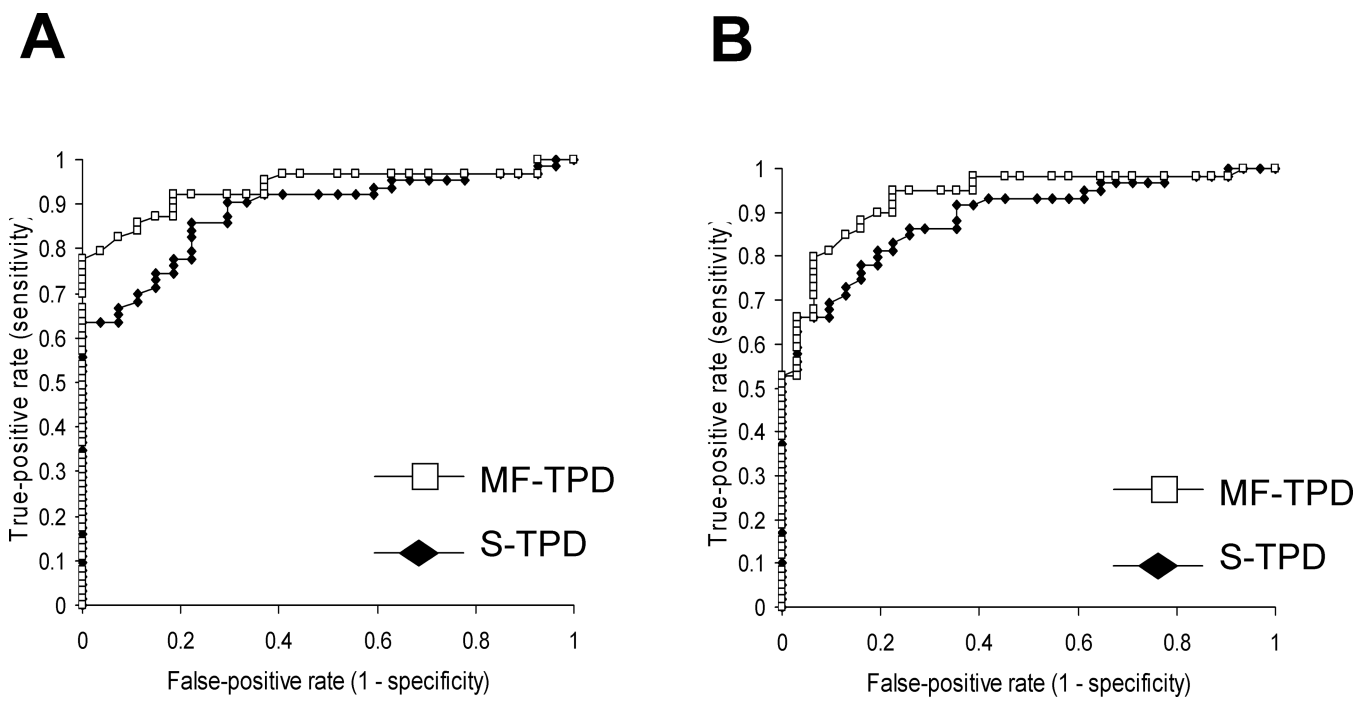

Figure 2.
ROC curves for detection of ≥50% stenosis (A) and ≥70% stenosis (B) by measures of S-TPD and MF-TPD in obese patients (n=90).

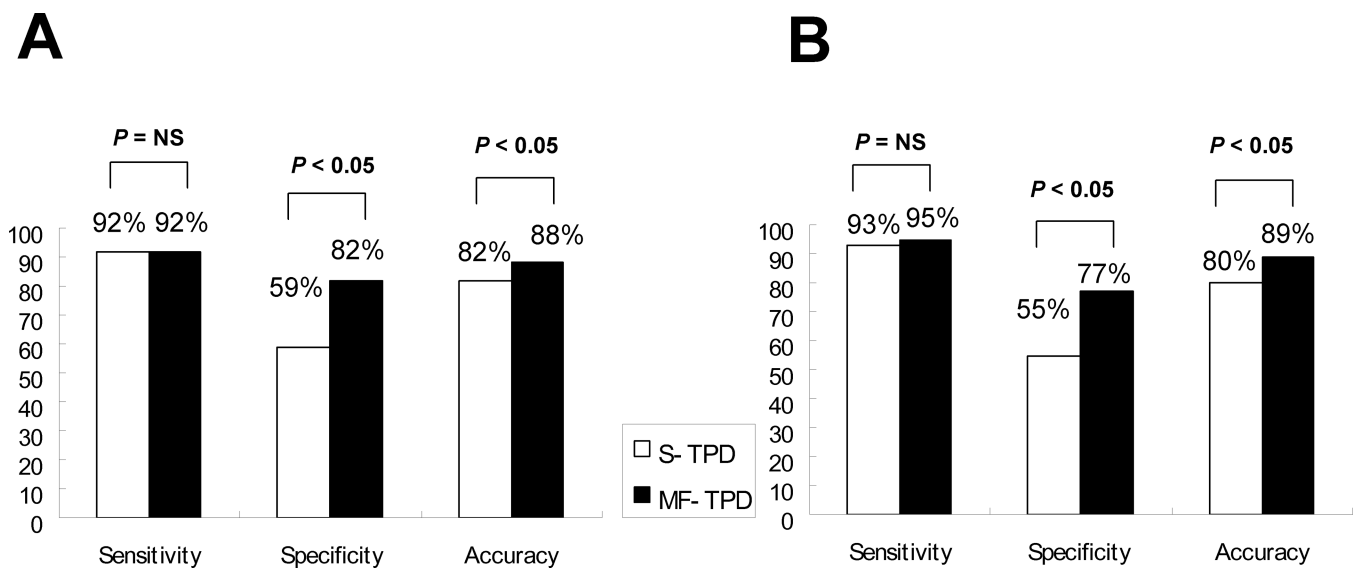

Figure 3.
Sensitivity, specificity and accuracy for detection of CAD with ≥50% stenosis criterion (A) and ≥70% stenosis criterion (B) by S-TPD and MF-TPD in obese group.

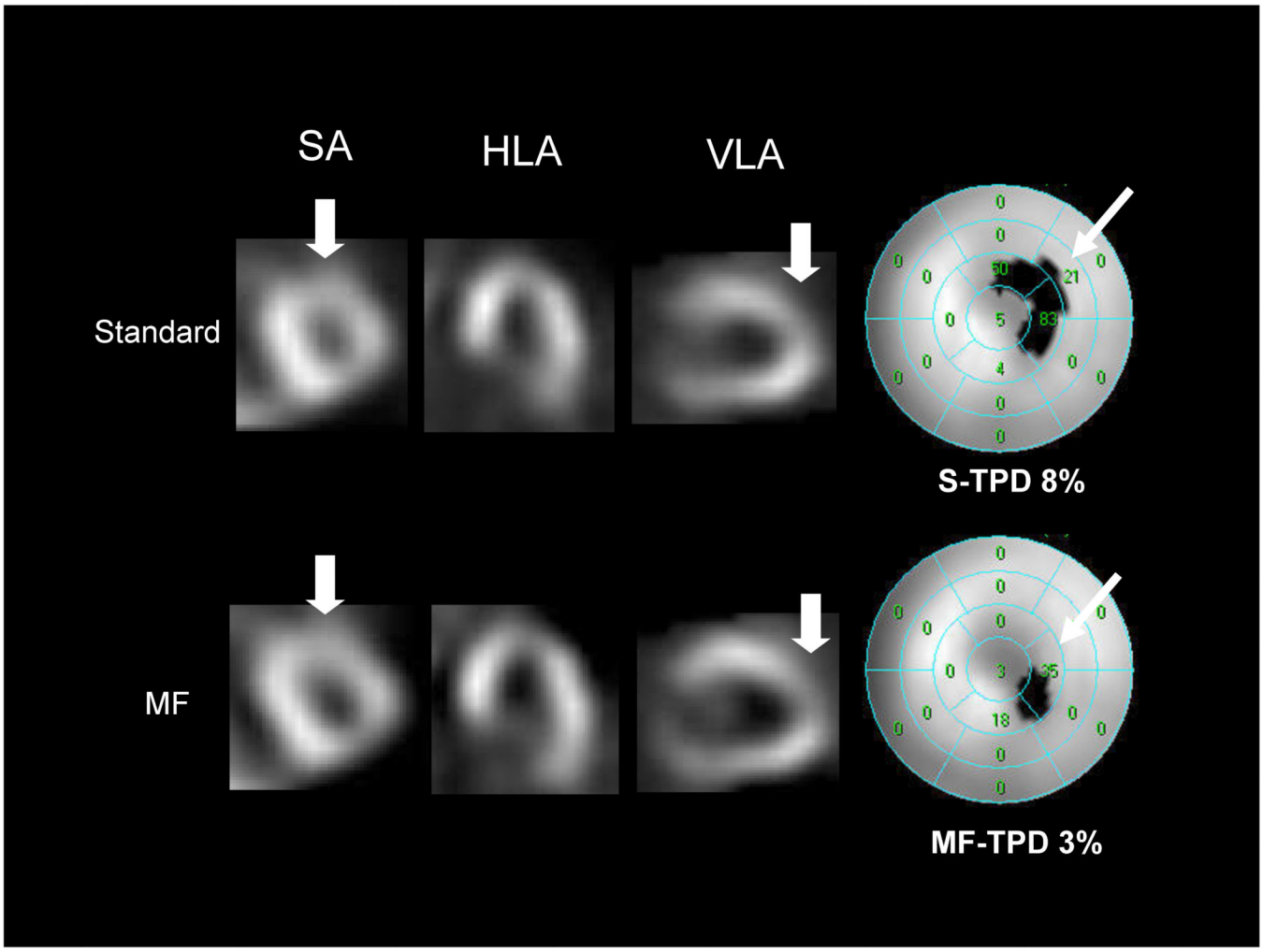

Figure 4.

Examples of false positive adenosine stress standard summed perfusion results corrected by motion-frozen analysis in a 68-year old asymptomatic woman with hypertension, hypercholesterolemia and ST depression during adenosine stress. Subsequent coronary angiogram showed no significant stenosis. Her left ventricular ejection fraction (LVEF) at stress was 76%. Shown are selected tomograms in the distal (apical) short axis (SA), mid horizontal long axis (HLA), mid vertical long axis (VLA). MF perfusion images appear larger than the standard summed images because they are reconstructed in the end diastolic position. MF images show brighter anterior and lateral wall from base to mid segments compared to standard perfusion images. On the VLA and SA, MF images show brighter distal anterior wall than standard summed image while MF images show count reduction in the apex potentially due to anatomical apical thinning. Quantitative analysis (right) shows insignificant apical thinning on motion-frozen MPS (TPD 3%) and significant defect in the same location on standard MPS data (TPD 8%).

TABLE 1

Characteristics of patients with a low likelihood of CAD used for creation of the database

Parameter	Value (n=80)
Age	56±14
Sex (female)	40 (50%)
BMI *	27±5
Hypertension	39 (49%)
Hypercholesterolemia	44 (55%)
Smoking	2 (3%)
Exercise test	57 (71%)

* BMI=Body Mass Index (kg/m^2)

TABLE 2

Characteristics of the obese patients comprising the study population

Parameter	Value (n=90)
Age	63±12
Sex (female)	27 (30%)
BMI	34.3±3.6
Hypertension	67 (74%)
Diabetes	36 (40%)
Hypercholesterolemia	45 (50%)
Symptoms Asymptomatic	15 (17%)
Nonanginal chest pain	8 (9%)
Atypical angina	36 (40%)
Typical angina	14 (16%)
Shortness of breath	9 (10%)
Exercise stress	45 (50%)

TABLE 3

Angiographic Characteristics

Parameter	Value (n=90)
≥70% stenosis	59 (66%)
≥50% stenosis	63 (70%)
Single-vessel disease *	29 (32%)
Double-vessel disease *	16 (18%)
Triple-vessel disease *	14 (16%)

* Based on 70% stenosis criterion

TABLE 4

Average stress TPD measurements in the study population by angiographic result

	S-TPD	MF-TPD	P value
No CAD* (n=31)	5.2±3.4%	3.9±2.6%	P=0.0003
CAD* (n=59)	15.9±9.1%	14.1±7.9%	P<0.0001

*≥70% stenosis

TABLE 5

Areas under the ROC curves for detection of ≥50% and ≥70% stenosis by S-TPD and MF-TPD in 90 obese patients

	ROC area under curve (±SD)	
Method	≥50% stenosis	≥70% stenosis
S-TPD	0.88±0.33	0.89±0.32
MF-TPD	0.94±0.24 *	0.93±0.25 *

* Significantly better ($p<0.05$) than S-TPD

TABLE 6

Diagnostic performance of S-TPD and MF-TPD for detection of ≥50% stenosis in 90 obese patients

	TP	TN	FP	FN
S-TPD	58	17	11	5
MF-TPD	58	23	5	5

TP: true positive, TN: true negative, FP: false positive, FN: false negative

TABLE 7

Diagnostic performance of S-TPD and MF-TPD for detection of ≥ 70% stenosis in 90 obese patients

	TP	TN	FP	FN
S-TPD	55	17	14	4
MF-TPD	56	24	7	4

TABLE 8

Patient characteristics of the cases who had false positive S-TPD corrected by MF-TPD for detection of ≥ 70% stenosis

Patient	age	sex	S-TPD %	MF-TPD %
HJ	62	Male	7	3
RA	88	Male	6	3
LD*	68	Female	8	3
HD	66	Female	6	3
RR	56	Male	6	4
SI	60	Male	10	4
WL	76	Male	7	4

*True positive for S-TPD for detection of ≥ 50% stenosis